

Numerical Model for Vaporization Simulation of a Single Droplet

S. Torfi, S. M. Hosseini Nejad

Abstract— A numerical model is developed in this study to simulate single droplet heat and mass transfer in saturated solvent vapor environment by finite volume method and transient SIMPLEX algorithm in spherical coordinates system. In this model, for simulation of the mass transfer, dimensionless equations of motion, heat transfer and mass transfer are solved simultaneously. The numerical analysis results are presented for mass transfer of lithium bromide solution droplet in 300K and initial concentration of 50%. Verification of method is done by compare these numerical results with analytical and numerical analysis of other studies. Droplet Growth Chart, average temperature and concentration, variation of drag coefficient diagrams, Nusselt number and flow line, temperature and concentration and temperature distribution contours, penetration rate of mass and the level of tangential velocity at droplet surface as the modeling results are presented.

Keywords— Numerical Model, CFD, Heat and Mass Transfer, Finite Volume Method, Droplet, Variable Properties.

NOMENCLATURE

A	Area
c_p	Specific Heat at Constant Pressure
Ca	Capillarity Number
C_p	Pressure Drag Coefficient
C_f	Frictional Drag Coefficient
C_T	Thrust Drag Coefficient in (Suction Or Discharge)
C_D	Overall Drag Coefficient
D	Diameter
k	Thermal Conductivity
L	Latent Heat of Vaporizing
m	Droplet Mass
\dot{m}_0^*	Inlet/Outlet Local Mass Rate of Droplets
Nu	Nusselt Number
P	Pressure
Pr	Prandtl Number

R	Radius
Re	Reynolds Number
S_C	Source Term at Continuity Equation
S_E	Source Term at Energy Equation
S_{RM}	Source Term at Radial Momentum Equation
S_{TM}	Source Term at Environmental Momentum Equation
S_w	Ambient Mass Transfer Equation
t	Time
T	Temperature
U_∞	Droplet Velocity at Free Flow
U_s	Maximum Vortex Velocity inside the Droplet
V	Non Dimensional Velocity in the Free Flow of Droplet
V	Volume
w	Concentration (Mass Ratio)
We	Weber Number
Γ_ϕ	General Transfer Coefficient
θ	Angular Coordinate
ϕ	General Variable
ρ	Density
σ	Surface Tension
τ	Shear Stress
v	Velocity

I. INTRODUCTION

In Industrial processes such as fuel injection, cooling fluids in cooling towers, most of the drying solution and many other industrial processes, droplet behavior considered one of the important parameters in system design. The effect of droplets and bubbles in many industrial and natural processes is known for most of Engineers and researchers in different fields. Therefore modeling of hydrodynamic and thermal behavior of droplets and small fluid particles has been studied by many researchers in last decades. The phenomenon of heat and mass transfer, which is driven by

Sadegh Torfi, Department of Mechanical Engineering, Islamic Azad University Susangerd Branch, Susangerd, Iran (e-mail: st@siau.ac.ir).

Seyed Mohammad Hosseini Nejad, Department of Mechanical Engineering, Islamic Azad University Susangerd Branch, Susangerd, Iran (e-mail: hosseyini@hotmail.com).

the concentration gradient of chemical species, can easily be captured for a homogeneous system by solving the convection–diffusion equations for species and product. However, in the case of heterogeneous reactions in laminar flows we first need to track the position of the interface between the dispersed phase and the continuous phase and then solve the convection–diffusion equations in order to study mass transfer across the interface. There are various computational methods available in the literature to model multi-phase flows

Prakash and Sirignano studied an analytical solve of mass transfer from single one-partial droplet [1]. Haywood et al. presented numerically analysis to solve this problem [2]. Jazayeri and Hosseini Nejad studied droplet evaporation and condensation in steam environment with numerical simulations in above studies, equations of motion and energy in droplet and surroundings are resolved [3]. Numerical modeling of mass transfer with multi-pieces environment was studied by Chang et al. for first time with solving equations of motion, energy and concentration [4].

Torfi et al. [7] developed Numerical model for simulation two-pieces droplet. Salmanzadeh et al. [8] and Novieri et al. [8] and [9] very tried to continue their work but they could not. In this model the fluid in droplet was considered as single-phase surrounding steam as two-pieces in this study, the mass transfer from multi-piece droplet in single-pieces environment has been studied. Perform the important assumptions in this model can be assumed laminar flow, the droplets remain spherical and using the thermodynamic equilibrium level member noted. Thermodynamic properties concentration has been considered as a function of temperature.

II. GOVERNING EQUATIONS

Considering the mentioned assumptions, the equations of problem is as follows.

A. Mass Conservation

$$\frac{\partial \rho}{\partial t} = -(\vec{\nabla} \cdot \rho \vec{v}) \quad (1)$$

B. Momentum Conservation

$$\rho \frac{D\vec{v}}{Dt} = -\vec{\nabla} P - [\vec{\nabla} \cdot \vec{\tau}] \quad (2)$$

C. Distribution of Chemical Component A inside the Droplet

$$\frac{\partial(\rho w_A)}{\partial t} + (\vec{\nabla} \cdot \rho w_A \vec{v}) = (\vec{\nabla} \cdot \rho D_{AB} \vec{\nabla} w_A) \quad (3)$$

D. Energy Conservation around Droplet

In the absence of energy source and sink, and regardless of the effects of radiation heat transfer and compressibility and viscosity, the energy equation the problem assuming thermal conductivity from Fourier law, is written as follows:

$$\frac{\partial}{\partial t}(\rho T) + \vec{\nabla} \cdot (\rho \vec{v} T) = \vec{\nabla} \cdot \left(\frac{k}{c_p} \vec{\nabla} T \right) + S_E \quad (4)$$

$$S_E = \frac{k}{c_p^2} (\vec{\nabla} P \cdot \vec{\nabla} c_p) \quad (5)$$

E. Internal Energy Conservation in Droplet

$$\frac{\partial}{\partial t}(\rho T) + \vec{\nabla} \cdot (\rho \vec{v} T) = \vec{\nabla} \cdot \left(\frac{k}{c_p} \vec{\nabla} T \right) + S_E \quad (6)$$

$$S_E = \frac{k}{c_p^2} (\vec{\nabla} P \cdot \vec{\nabla} c_p) + \frac{1}{C_p} \frac{\partial h}{\partial w} \Big|_{p,T} [\vec{\nabla} \cdot \rho D_{AB} \vec{\nabla} w] \quad (7)$$

III. BOUNDARY CONDITIONS

A. Symmetric Boundary Conditions

The boundary is symmetry axis of problem, where the boundary conditions are:

$$\left. \frac{\partial \phi}{\partial \theta} \right|_{\theta=0, \theta=\pi} = 0, \quad \phi = v_r, T, w \quad (8)$$

$$v_\theta = 0$$

B. Free Flow Boundary Condition

This boundary consists of two parts; inlet and outlet of flow at inlet ($0 \leq \theta \leq \pi/2$ And $r = r_\infty$) Velocity and temperature values can be assumed equal to their values in free flow. Boundary condition at output flow ($\pi/2 < \theta \leq \pi$ And $r = r_\infty$) could be assumed as zero radial gradient.

C. Liquid-Gas Common Surface

For derive common surface boundary condition, integrate the control volume equations that surrounds common surface that limit to zero the details of the boundary conditions derivation for the radial velocity is given in Ref [5]

Radial velocity of liquid:

$$v_{r,l,S} = \frac{\dot{m}_0^*}{\rho_{l,S}} + \frac{dR}{dt} \quad (9)$$

Radial velocity of vapor phase:

$$v_{r,g,S} = \frac{\dot{m}_0^*}{\rho_{g,S}} + \frac{dR}{dt} \quad (10)$$

Shear stress conservation at the level of:

$$\tilde{\tau}_{r\theta,l} = \tilde{\tau}_{r\theta,g} \quad (11)$$

Boundary condition equations for concentration and temperature in common surface is more complex. Mass Penetration to droplet is associated with the energy release due to phase change. Boundary condition equations of problem in common surface relative vapor exchange between the environment and droplet. In Common surface,

for achieve to consistent thermal boundary condition, thermodynamic equilibrium assumption is used. This means that temperature of droplet surface is considered equal to fluid saturation temperature (at local pressure and concentration).

$$P_S^0 = P_g^0 + \Delta P_\sigma \quad (12)$$

$$\Delta P_\sigma = \sigma \cdot \left(\frac{2}{R^2} \right) \quad (13)$$

$$T_{g,S} = T_{l,S} = T_{SAT} \quad @ \quad w_S, P_S \quad (14)$$

Using energy conservation condition:

$$-k \frac{\partial T}{\partial r} \Big|_l = -k \frac{\partial T}{\partial r} \Big|_g + \dot{m}_0'' L \quad (15)$$

Calculations of concentration at droplet surface are as follows.

According to Fick law:

$$\rho_A (v_A - v) = -\rho D_{AB} \bar{\nabla} w_A \quad (16)$$

Where A and B are Chemical components in the fluid and velocities v And v_A Are calculated as follows.

$$v_A = \frac{\dot{m}_0''}{\rho_{l,A}} + \frac{dR}{dt} = \frac{\dot{m}_0''}{\rho_l w_A} + \frac{dR}{dt} \quad (17)$$

$$v_B = \frac{dR}{dt} \quad (18)$$

$$v = \frac{\dot{m}_0''}{\rho_l} + \frac{dR}{dt} \quad (19)$$

Thus if velocities v and v_A are known, concentration could be calculated with equation (16)

IV. NON-DIMENSIONING

In order to generalize the problem and presenting results in general dimensionless parameters, equations and boundary conditions must be non-dimensioned.

Define the dimensionless Variables

$$t = \frac{v_{\infty,0}^* t^*}{R_0^*} \quad r = \frac{r^*}{R^*(t)} \quad R = \frac{R^*(t^*)}{R_0^*} \quad T = \frac{T^*}{T_\infty^*}$$

$$v_r = \frac{v_r^*}{v_\infty^*(t)} \quad v_\theta = \frac{v_\theta^*}{v_\infty^*(t)} \quad V = \frac{v_\infty^*(t)}{v_{\infty,0}^*} \quad P = \frac{P^* - P_0^*}{\rho_\infty^* v_{\infty,0}^{*2}}$$

$$\rho = \frac{\rho^*}{\rho_\infty^*} \quad \mu = \frac{\mu^*}{\mu_\infty^*} \quad k = \frac{k^*}{k_\infty^*} \quad c_p = \frac{c_p^*}{c_{p,\infty}^*}$$

$$h = \frac{h^*}{c_{p,\infty}^* T_\infty^*} \quad L = \frac{L^*}{c_{p,\infty}^* T_\infty^*} \quad \dot{m}_0'' = \frac{\dot{m}_0^{*''}}{\rho_\infty^* v_{\infty,0}^*} \quad D_{AB} = \frac{D_{AB}^*}{D_{AB,0}^*}$$

A. Equations Non-Dimensioning

Conservation dimensionless equations form with dimensionless parameters defined before could be obtained in general form as:

$$\frac{\partial}{\partial t} (\rho V R \phi) + V^2 \bar{\nabla} \cdot \left\{ \rho \phi \left(v_r - \frac{r}{V} \frac{dR}{dt} \right) \hat{r} + v_\theta \hat{\theta} \right\} = \frac{V}{R} \bar{\nabla} \cdot (\Gamma_\phi \bar{\nabla} \phi) + S_\phi \quad (20)$$

In this equation ϕ General variable, Γ_ϕ and distribution coefficient and S_ϕ is source term String replace And Conservation equations for each Table 1 is shown. Replaced terms ϕ and Γ_ϕ for each conservation equation are shown in table 1. Conservation Equation of this case, not inherently include source term S_ϕ and it is appeared Because of selected dimensionless parameters and inclusion of equations in the overall form appearance is above. Noticeable point is that in second sentence, the time derivative of droplet radius is used in equation and modified velocity vector are shown as $(v_r - \frac{r}{R} \frac{dR}{dt}) \hat{r} + v_\theta \hat{\theta}$.

Reynolds Number:

$$Re_0 = 2 \rho_\infty^* v_{\infty,0}^* R_0^* / \mu_\infty^* \quad (1)$$

Prandtl Number:

$$Pr_\infty = \frac{c_{p,\infty}^* \mu_\infty^*}{k_\infty^*} \quad (2)$$

Schmitt Number:

$$Sc_0 = \frac{\mu_\infty^*}{\rho_\infty^* D_{AB,0}^*} \quad (3)$$

B. Non-Dimensioning Boundary Conditions

The dimensionless form of Boundary conditions of symmetric axis, droplet center and free flow are similar to dimensional form.

1) Boundary conditions at common surface

Dimensionless form of boundary conditions in common surface has difference to dimensional form

Radial velocity (liquid phase):

$$v_{r,l,S} = \frac{1}{V} \left\{ \frac{\dot{m}_0''}{\rho_{l,S}} + \frac{dR}{dt} \right\} \quad (4)$$

Radial velocity (gas phase):

$$v_{r,g,s} = \frac{1}{V} \left\{ \frac{\dot{m}_0''}{\rho_{g,s}} + \frac{dR}{dt} \right\} \quad (5)$$

Continuity of shear stress:

$$\tilde{\tau}_{r\theta,l} = \tilde{\tau}_{r\theta,g} \quad (6)$$

Conservation of energy:

$$-k \frac{\partial T}{\partial r} \Big|_{l,\theta} = -k \frac{\partial T}{\partial r} \Big|_{g,\theta} + \frac{\text{Re}_0 \text{Pr}_\infty R}{2} \dot{m}_0'' L \quad (7)$$

Known concentration at surface

$$w_A (v - v_A) = \frac{2}{\text{Re}_0 \text{Sc}_0} \frac{D_{AB}}{RV} \nabla w_A \quad (8)$$

$$v_A = \frac{1}{V} \left\{ \frac{\dot{m}_0''}{\rho_l w_A} + \frac{dR}{dt} \right\} \quad (9)$$

Relationship of the average and local Nusselt number and drag coefficient (friction, pressure, and overall thrust) also are written as follows. (All expressions are written in vapor phase)

$$Nu_g(\theta) = \frac{2k \frac{\partial T}{\partial r} \Big|_{r=1}}{(1 - T_s)} \quad (10)$$

$$\overline{Nu}_g = \frac{\int_0^\pi Nu_g(\theta) dA \Big|_{r=1}}{\int_0^\pi dA \Big|_{r=1}} \quad (11)$$

$$C_F = \frac{4}{\pi \text{Re}_0 RV} \int_0^\pi (\tilde{\tau}_{r\theta} \sin \theta - \tilde{\tau}_{rr} \cos \theta) dA \Big|_{r=1} \quad (12)$$

$$C_P = \frac{2}{\pi V^2} \int_0^\pi P \cos \theta dA \Big|_{r=1} \quad (13)$$

$$C_T = \frac{2}{\pi} \int_0^\pi \rho v_r^2 \cos \theta dA \Big|_{r=1} \quad (14)$$

Thrust drag component is due to asymmetric evaporation and condensation on the surface droplet.

V. NUMERICAL MODEL AND VALIDATION

In order to solve highly coupled equations, finite volume method and SIMPLEC algorithm is used. With integration of equations on the control volume element in time ranged, discrete form of equations are obtained that with using the algorithm SIMPLEC and moved Network could be solved in transient form. Computation is done in a network with 1500 (50 * 30) elements in droplet and 2500 (50 * 50) elements outside of droplets and forwarding speed of 1e-6sec that written by Visual C++ programming language including 67

sub programs. More details and explanations are available in Ref [5].

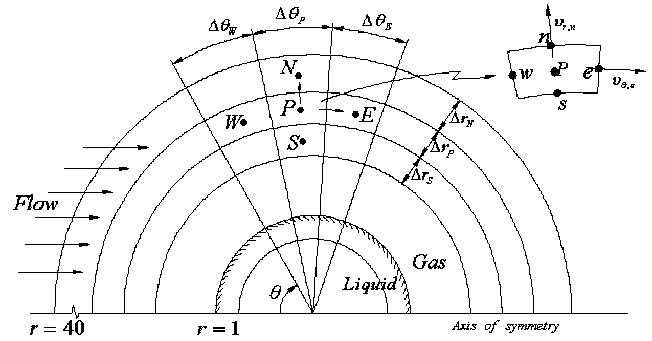


Fig 1. Flow Field Networking.

After investigations and solve the flow around solid sphere and around a liquid droplet flow, SIMPLEC algorithm was chosen due to its convergence time less than the SIMPLE algorithm then all Modeling is presented in SIMPLEC algorithm. For select suitable Discrete method, isothermal flow around a solid sphere is solved by code written by this study and Fluent code separately that in both code, weakness of upwind different and hybrid methods was evident. On the other hand, the modified central difference method solve is greatly accordance with results of solve obtained with the precise second order methods Fluent code and experimental results were. Thus the analysis performed by the modified central difference method is used. In the analysis, isothermal flow around a solid sphere solution in performed in different Reynolds numbers and drag coefficient, and vortex behind the sphere and Vortex separation point in the this analysis and other numerical and experimental results are compared. For isothermal flow around a spherical drop, analytical relations presented by Clift et al. to calculate the drag force has been comparing with results of this study [6]. Also a Comparison is done between parameters of isothermal air flow around a droplet of water in the present analysis and results reported by LeClair & Hamielec [7] and Haywood et al. [2] that shown reasonably compliant as shown in Table 1. In Fig. 2 evaporation of water droplet at uniform temperature 320K, Radius 0.5mm and initial Re 100 at superheated water vapor at 340K and 10kPa is shown and in Fig. 3 variation of average Nu for Evaporation of water droplet is compared. Condensation of water vapor on a water droplet with uniform temperature 310K, Radius 0.5mm and initial Re 100 at superheated water vapor at 350K and 40kPa is shown in Fig. 4 and in Fig. 5 comparison of variation of CD for condensation of water vapor on a water droplet is shown. Fig. 6 showed absorption of water vapor by a Li-Br droplet at uniform initial temperature 320K, Radius 0.5mm and initial Re 100 at superheated water vapor at 320K and in Fig. 7 comparison of variation of CD as function of times for absorption of water vapor by a Li-Br droplet is shown.

Table 1. Comparison of isothermal parameters of air flow around water droplet.

$\mu_l / \mu_g = 55$		Present result	Haywood et al.[2]	LeClair & Hamielec
Re=100	C_p	0.513	0.511	0.49
	C_F	0.578	0.578	0.59
	C_D	1.091	1.09	1.08
	$v_{l,MAX}$	0.035	0.036	0.037
	$\theta_{v_l,MAX}$	67	64	69

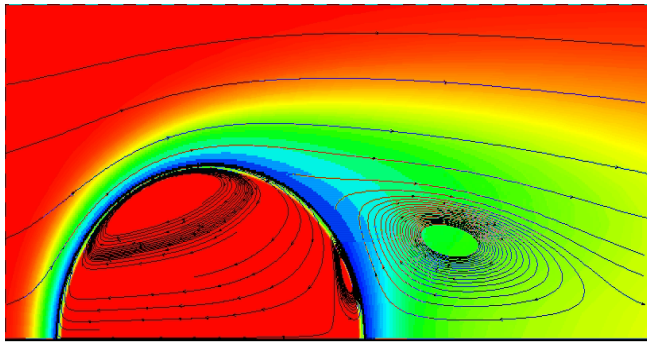


Fig 2. Evaporation of water droplet at uniform temperature at superheated water vapor.

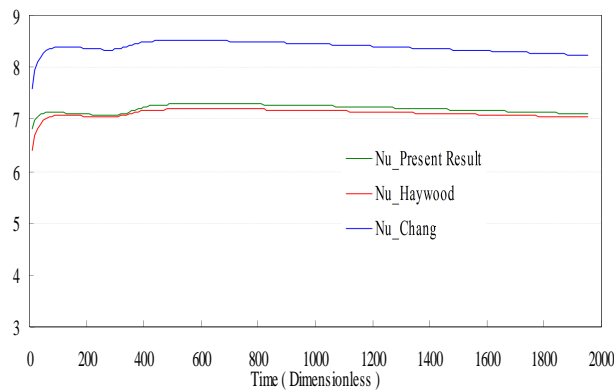


Fig 3. Comparison of variation of Average Nusselt number for Evaporation of water droplet.

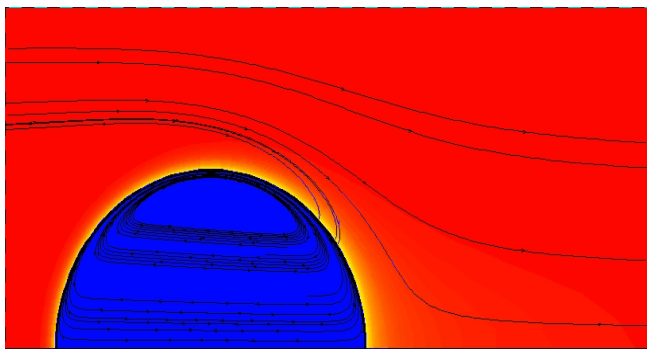


Fig 4. Condensation of water vapor on a water droplet with uniform temperature at superheated water.

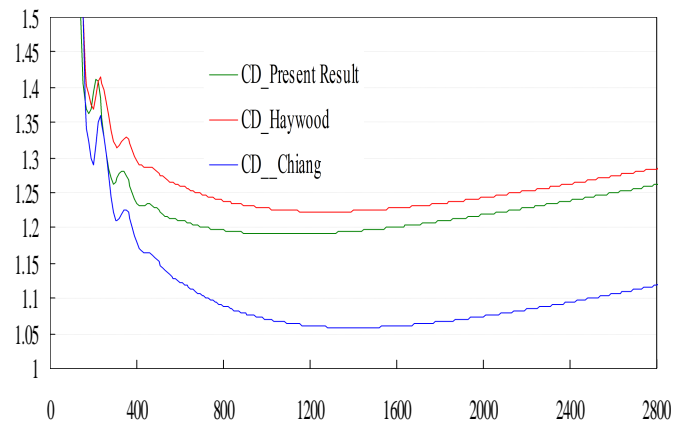


Fig 5. Comparison of variation of CD condensation of water vapor on a water droplet.

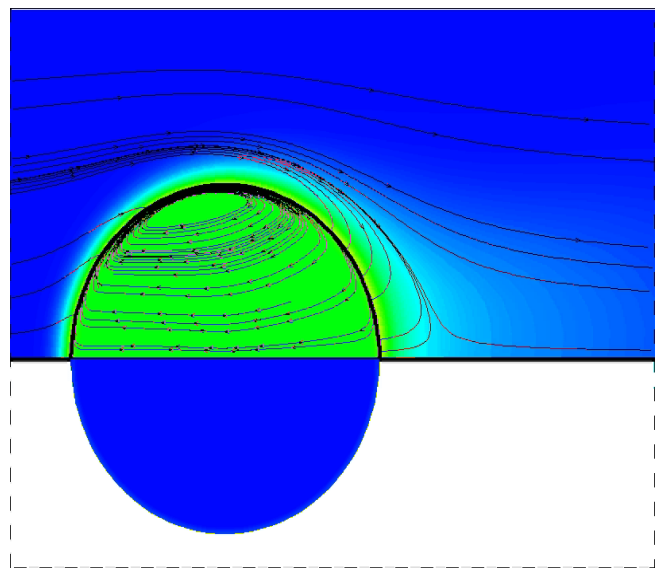


Fig 6. Absorption of water vapor by a Li-Br droplet at uniform temperature at superheated water vapor.

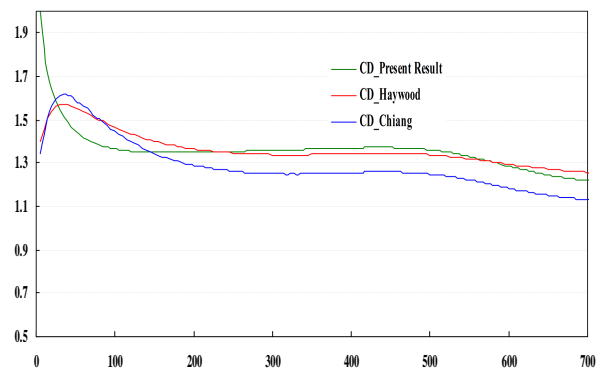


Fig 7. Comparison of variation of CD for absorption of water vapor by a Li-Br droplet.

VI. CONCLUSIONS

The results of numerical analysis are presented for mass transfer of lithium bromide solution droplet in 300K and initial concentration of 50%.

In figure 8, surface temperature and distribution in droplets surface at 6 different times is plotted. Temperature boundary conditions on droplet surface is depends on pressure and is function of droplet's absorption rate of vapor and also absorption rate of vapor depends on surface temperature and its neighbors. On the other hand, the surface pressure obtained from velocity profiles around droplets Because of high suction on the surface of droplet, velocity profile and thus the surface pressure distribution has also changed. Thus adsorption is function of three important parameters; pressure, temperature and surface concentration that in this case the three parameters strongly depend on each other. In figures 8 and 9 high dependency between these three parameters is shown. The overall drag coefficient that consist of three components pressure drag, friction and thrust drag, is decreases in initial moments and then Start to increase after reaching the minimum point at approximately $t=150s$, But pressure and thrust drag increase in initial moments and then after reaching maximum point approximately $t=50s$ are starting to decrease. As shown in Figure 4, the major component of drag in absorption process of droplet is frictional drag component Frictional drag component in the initial moments is too high due to high vacuum pressure of droplet and too low thickness of boundary layer on droplet surface , and then become steady state with decreasing suction rate. In figures 10 and 11, constant temperature and concentration lines at four different times is plotted. As could be seen in Figures, concentration penetration power is much weaker than temperature and concentration boundary layer formed in droplet surface is very thin.

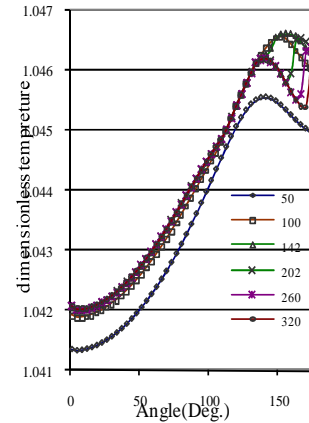


Fig. 8: Distribution of Droplet's Surface Temperature

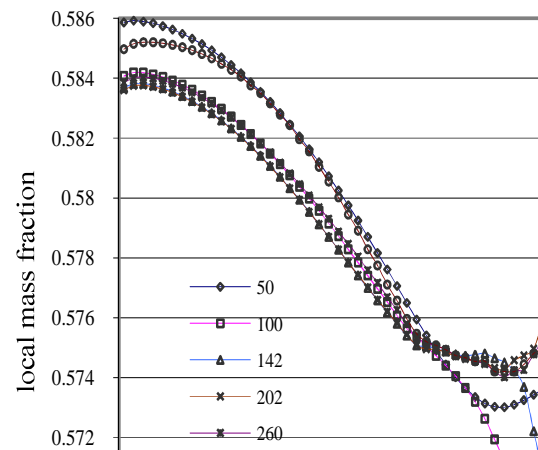


Fig. 9: Solution Mass Ratio at Droplet Surface

Table 1, General Parameters Definition

Equation	ϕ	Γ_ϕ	S_ϕ
Continuity	1	0	S_C
Radial Momentum	v_r	$\frac{2\mu}{Re_0}$	S_{RM}
Tangential Momentum	v_θ	$\frac{2\mu}{Re_0}$	S_{TM}
Energy	T	$\frac{2k}{c_p Re_0 Pr_\infty}$	S_E
Species	w	$\frac{2\rho D_{AB}}{Re_0 Sc_0}$	S_w

Where;

$$S_C = \rho R \frac{dV}{dt} - 2\rho V \frac{dR}{dt}$$

$$S_{RM} = V^2 \left\{ \vec{\nabla} \cdot (\rho \vec{v} v_r) - \vec{\nabla} \cdot (\rho \vec{v} \vec{v})_r \right\} - \frac{2V}{Re_0 R} (\vec{\nabla} \cdot \mu \vec{\nabla} v_r - (\vec{\nabla} \cdot \vec{\tau})_r) - 2\rho V v_r \frac{dR}{dt} - \frac{\partial P}{\partial r}$$

$$S_{TM} = V^2 \left\{ \vec{\nabla} \cdot (\rho \vec{v} v_\theta) - \vec{\nabla} \cdot (\rho \vec{v} \vec{v})_\theta \right\} - \frac{2V}{Re_0 R} (\vec{\nabla} \cdot \mu \vec{\nabla} v_\theta - (\vec{\nabla} \cdot \vec{\tau})_\theta) - 2\rho V v_\theta \frac{dR}{dt} - \frac{\partial P}{\partial \theta}$$

$$S_E = \rho TR \frac{dV}{dt} - 2\rho TV \frac{dR}{dt} + \frac{2V}{Re_0 Pr_\infty R} \frac{k}{c_p^2} (\vec{\nabla} T \cdot \vec{\nabla} c_p) \quad \text{around droplet}$$

$$S_E = \rho TR \frac{dV}{dt} - 2\rho TV \frac{dR}{dt} + \frac{2V}{Re_0 Pr_\infty R} \frac{k}{c_p^2} (\vec{\nabla} T \cdot \vec{\nabla} c_p) + \frac{V}{R} \vec{\nabla} \cdot (\Gamma_w \vec{\nabla} w) \quad \text{inside droplet}$$

$$S_w = \rho w R \frac{dV}{dt} - 2\rho w V \frac{dR}{dt} \quad \text{inside droplet}$$

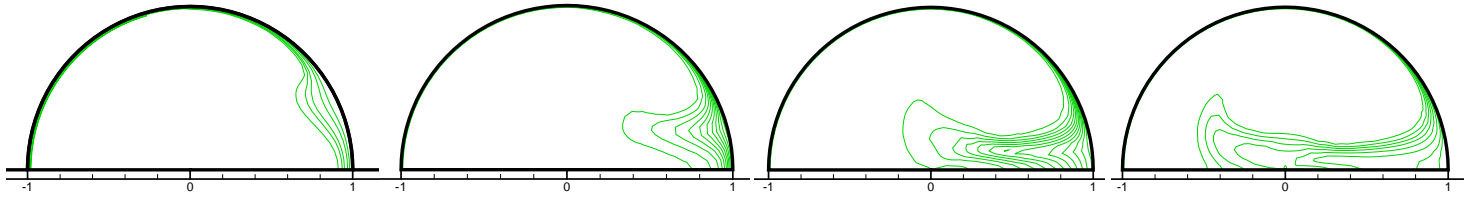


Fig. 10: Constant Temperature Lines for Various Times

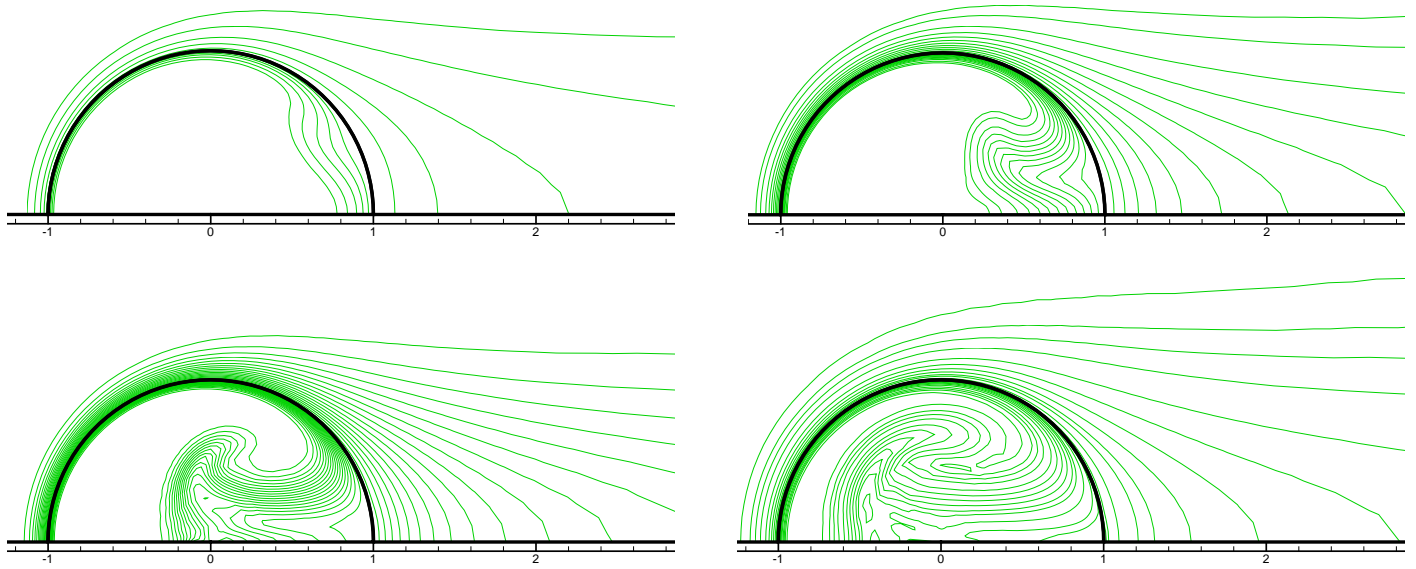


Fig. 11: Constant Concentration Lines for Various Times.

REFERENCES

- [1] Prakash , S., Sirignano, W. A., (1980), "Theory of convective droplet vaporization with unsteady heat transfer in the circulating liquid phase ", *Int. J. Heat Mass Transfer*, Vol. 23, pp. 253-268.
- [2] R. J. Haywood, N. Nafziger & M. Renksizbulut, (1989), "A detailed examination of gas and liquid phase transient processes in convective droplet evaporation ", *ASME J. Heat Transfer*, Vol. 111, pp.495-502.
- [3] Jazayeri, S. A., Hoseini Nejad, S. M., (2003), "Solving heat transfer and movement equations for single droplet with considering condensation and vaporization by finite element method", 11th int. conf. of mechanical engineering, vol. 2, pp 596-603, Iran.
- [4] Chang, C. H. Raja, M. S. , Sirignano, W. A. , 1992, " Numerical analysis of convecting , vaporizing fuel droplet with variable properties ", *Int. J. Heat Mass Transfer* , Vol. 35, pp.1307-1324.
- [5] Hoseini Nejad, S. M., (2003), "Numerical simulation of hydrodynamics, heat and mass transfer of two-pieces droplet" M.S. thesis, K.N. Toosi University of technology, Tehran, Iran.
- [6] Clift, R. , Grace, J. R., Weber, M. E., (1978), "Bubbles, Drops and particles", Academic press, USA.
- [7] S. Torfi, S. M. Hosseini Nejad, E. Novieri, K. Ogbi, (2010)"Simulation of Heat and Mass Transfer from a Droplet of Two-Pieces Solution with Solvent Vapor by the Finite Volume Method", 6th WSEAS International Conference on APPLIED and THEORETICAL MECHANICS, Athens, Greece.
- [8] M. Salmanzadeh, S. Torfi, S.R. Mosavifar, (2010)" Numerical Simulations of Transient Flow Occurrence in Pipelines by Appropriate Division Of The Pipeline Length Method", 6th WSEAS International Conference on APPLIED and THEORETICAL MECHANICS, Athens, Greece.
- [9] E. Novieri, S. Torfi, S.M. Hosseini Nejad, (2010)" Bit Run Optimization through Simulation: A Case Study", 6th WSEAS International Conference on APPLIED and THEORETICAL MECHANICS, Athens, Greece.
- [10] E. Novieri, S. Torfi, (2010)"Use Non-Rotating Adjustable Stabilizer to Optimize a Directional Drilling Plan", 6th WSEAS International Conference on ENERGY, ENVIRONMENT, ECOSYSTEMS and SUSTAINABLE DEVELOPMENT, Timisoara, Romania.